Supplemental Information

Supplementary figures and figure legends:

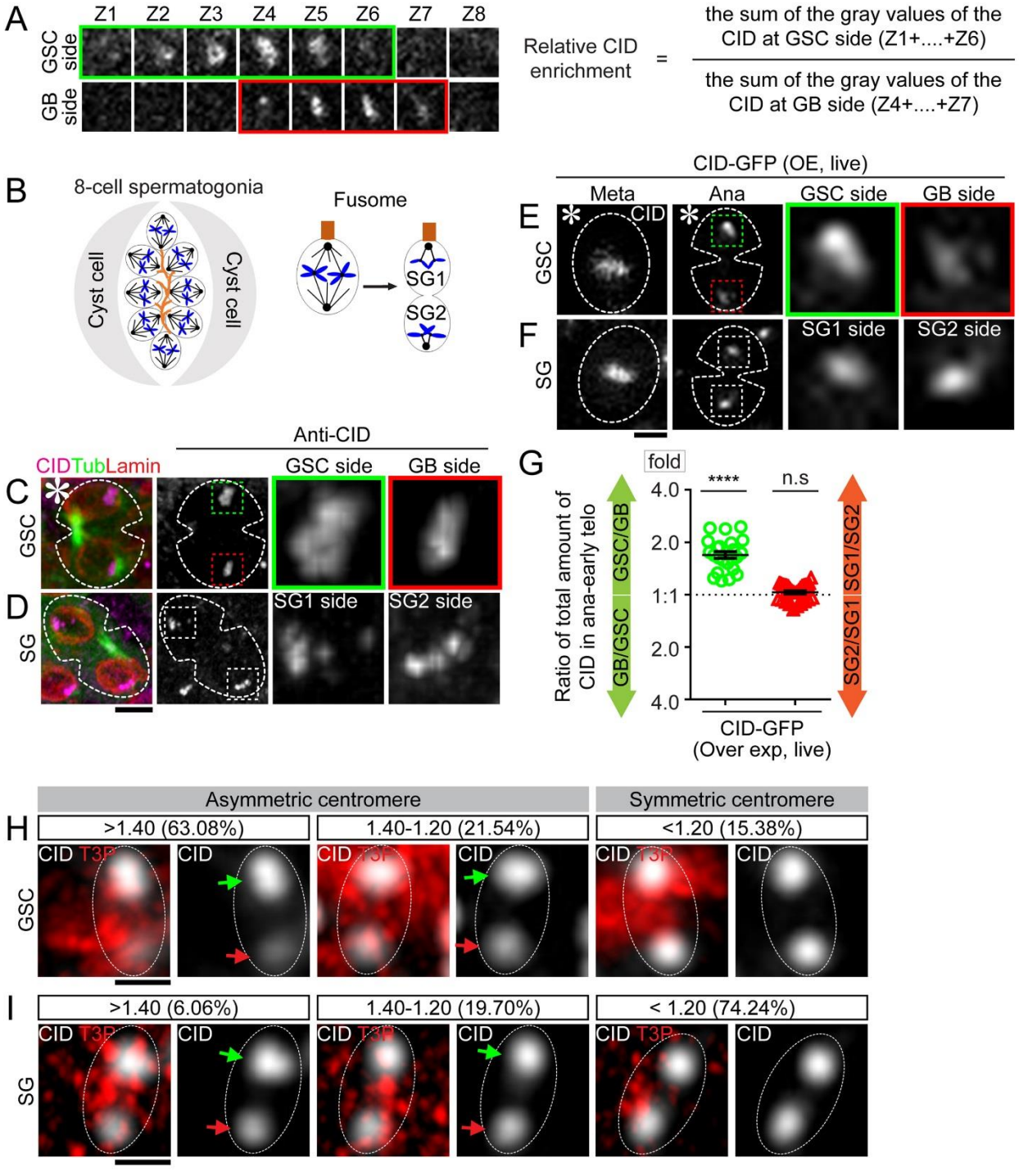

Figure S1. Related to Figure 1: Quantification of CID inheritance pattern in mitotic male germ cells. (**A**) Illustration of 3D quantification: total amount of CID toward GSC side or GB

side was obtained by summing CID signals from all slices with signals from a Z-stack, with background subtracted from each slice, for example, Z1 through Z6 from the GSC side and Z4 through Z7 from the GB side. The ratio was subsequently deducted by dividing the total amount of CID from GSC side by the total amount of CID from GB side. (**B**) A cartoon depicting symmetric spermatogonia cell (SG) division. Here SG1 is defined as the one in proximity to the fusome structure while SG2 is the one distal to the fusome. (**C-D**) Images of an early telophase GSC (**C**) and a SG at the same stage (**D**) from *nanos-Gal4*; *UAS-α-tubulin-GFP* testes, immunostained with anti-CID (magenta) and anti-Lamin B (red). (**E-F**) Snapshots from live cell imaging using a *cid-GFP* line, both metaphase and early anaphase were shown for a GSC (**E**) and a SG (**F**). Enlarged images show CID-GFP signals in the anaphase GSC in (**E**) and the anaphase SG in (**F**). (**G**) Quantification of CID-GFP at anaphase or early telophase GSCs and SGs, using method shown in (**A**): 1.73± 0.08-fold for GSC/GB (*n*= 23), 1.02± 0.02-fold for SG1/SG2 (*n*= 31), Table S3. (**H**) Examples of resolved individual sister centromeres in GSCs. In prometaphase GSCs, distribution patterns of CID at resolved individual sister centromeres showed different categories of asymmetry: highly asymmetric (> 1.40-fold, 63.1%) and medium asymmetric (between 1.2-1.4-fold, 21.5%), as well as symmetric pattern (<1.2-fold, 15.4%) in GSCs. Quantification also shown in Figure 1I-J (*n*= 65). (**I**) Examples of resolved individual sister centromeres in SGs. In prometaphase SGs, distribution patterns of CID at resolved individual sister centromeres showed different categories of asymmetry: highly asymmetric (> 1.40-fold, 6.1%) and medium asymmetric (between 1.2-1.4-fold, 19.7%), as well as symmetric pattern (<1.2-fold, 74.2%) in SGs. Quantification also shown in Figure 1I-J (*n*= 66). Ratio= Avg± SE; *P*-value: paired *t* test. ****: $P< 10^{-4}$; n.s: no significant difference from 1:1 ratio. Asterisk: hub. Scale bars: 2μm (**C-D**, **E-F**), 0.5μm (**H-I**).

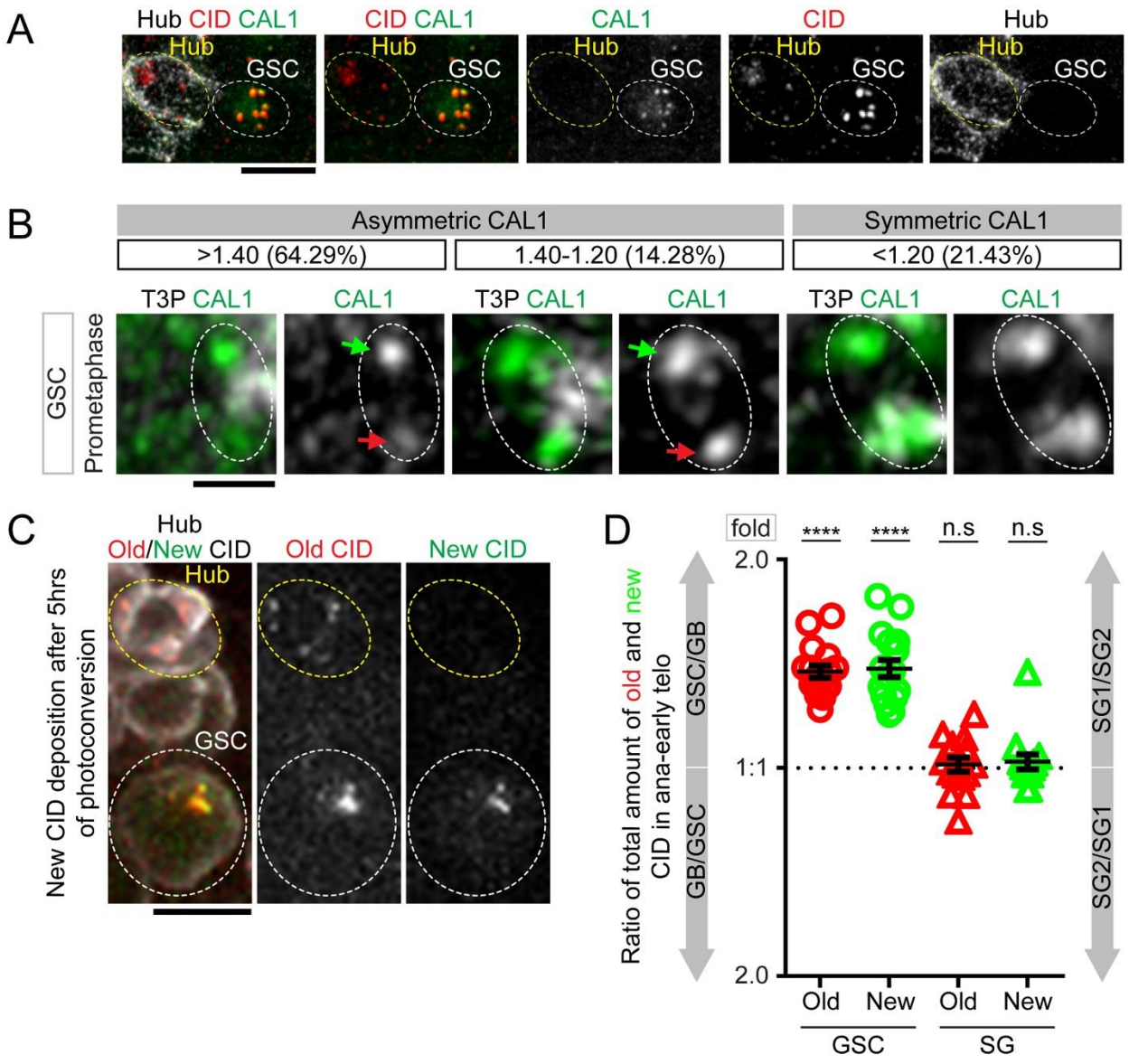

Figure S2. Related to Figure 2: CAL1 expression and inheritance patterns in male GSCs.

(**A**) Apical tip of a testis from *Dendra2-cal1* knock-in male fly: Dendra2-CAL1 (green) was detectable at centromeres and colocalized with CID (red) in GSCs, but was not detectable in non-replicative hub cells even though CID was detectable in hub cells, indicating specificity of CAL1 expression and localization in replicative cells, which is likely for new CID incorporation in preparation for cell divisions. (**B**) In prometaphase GSCs, distribution patterns of CAL1 at resolved individual sister centromeres showed different categories of asymmetry: highly

asymmetric (> 1.40-fold, 64.3%) and medium asymmetric (between 1.2-1.4-fold, 14.3%), as well as symmetric pattern (<1.2-fold, 21.4%) in GSCs. Quantification also shown in Figure 2E (*n*= 28). (**C**) After photoconversion, testes were cultured for 5hrs *ex vivo* before fixation. New CID (green Dendra2) incorporation is detectable in early prophase GSCs but not in non-replicative hub cells. (**D**) Quantification of old CID (red) and new CID (green) at approximately 15 hours after photoconversion in anaphase or early telophase GSCs and SGs: 1.38± 0.03-fold (old CID) and 1.40± 0.04-fold (new CID) for GSC/GB (*n*= 17), 1.02± 0.02-fold (old CID) and 1.01± 0.03-fold (new CID) for SG1/SG2 (*n*= 15). Ratio= Avg± SE; *P*-value: paired *t* test. ****: $P< 10^{-4}$; n.s: no significant difference from 1:1 ratio. Scale bars: 5μm (**A, C**) and 0.5μm (**B**).

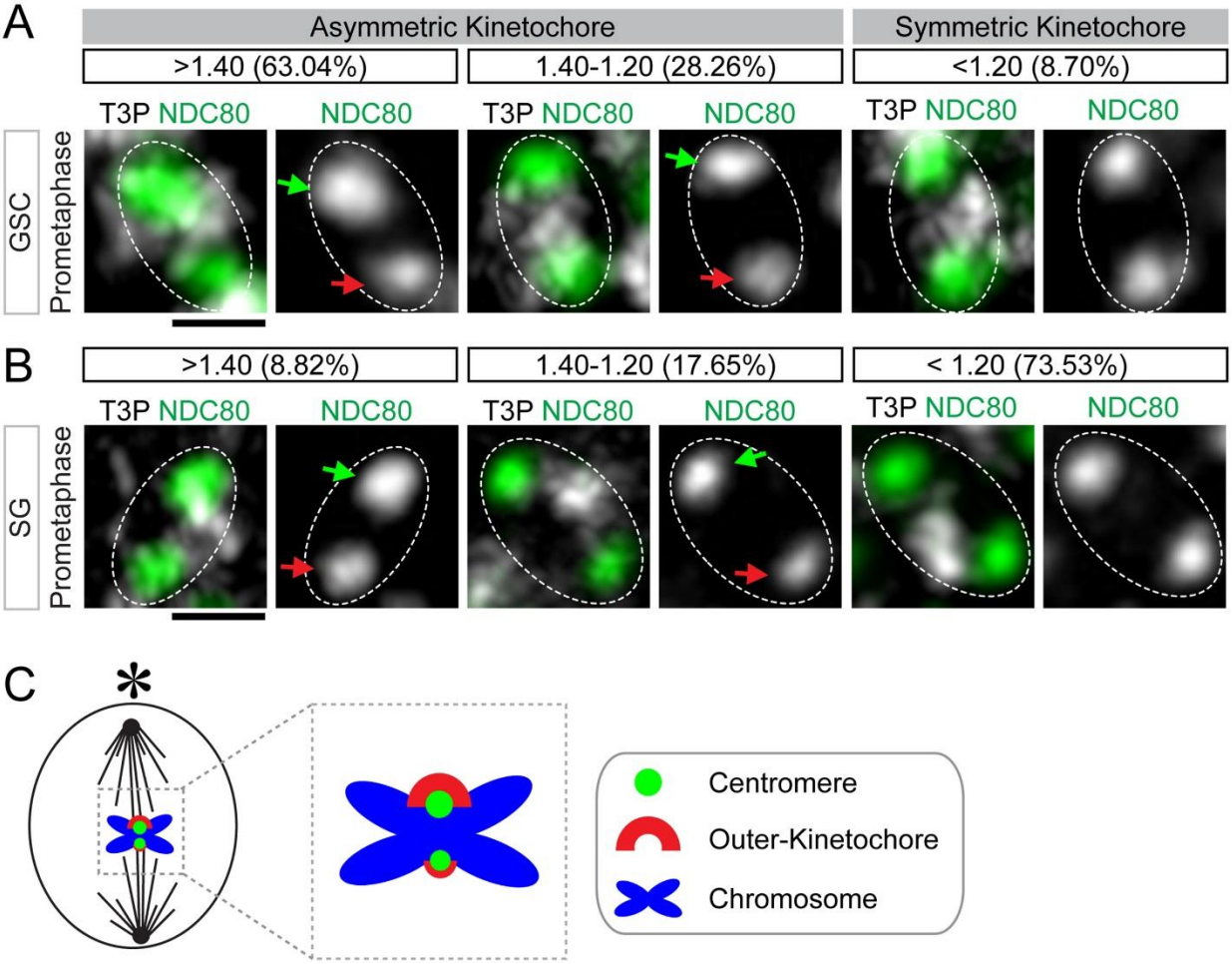

Figure S3. Related to Figure 3: Distribution of a key kinetochore protein NDC80 at sister kinetochores. (**A**) Examples of resolved individual sister kinetochores in prometaphase GSCs. Distribution of NDC80 at resolved individual sister kinetochores showed different categories of asymmetry: highly asymmetric (> 1.40-fold, 63.0%) and medium asymmetric (between 1.2-1.4-fold, 28.3%), as well as symmetric pattern (<1.2-fold, 8.70%) in GSCs. Quantification also shown in Figure 3F-G (*n*= 46). (**B**) Examples of resolved individual sister kinetochores in prometaphase SGs. Distribution of NDC80 at resolved individual sister kinetochores showed different categories of asymmetry: highly asymmetric (> 1.40-fold, 8.8%) and medium asymmetric (between 1.2-1.4-fold, 17.7%), as well as symmetric pattern (<1.2-fold, 73.5%) in

SGs. Quantification also shown in Figure 3F-G (*n*= 34). (**C**) A cartoon depicting the asymmetric sister centromeres correlate with different levels of NDC80 between sister kinetochores. Asterisk: hub. Scale bars: 0.5μm.

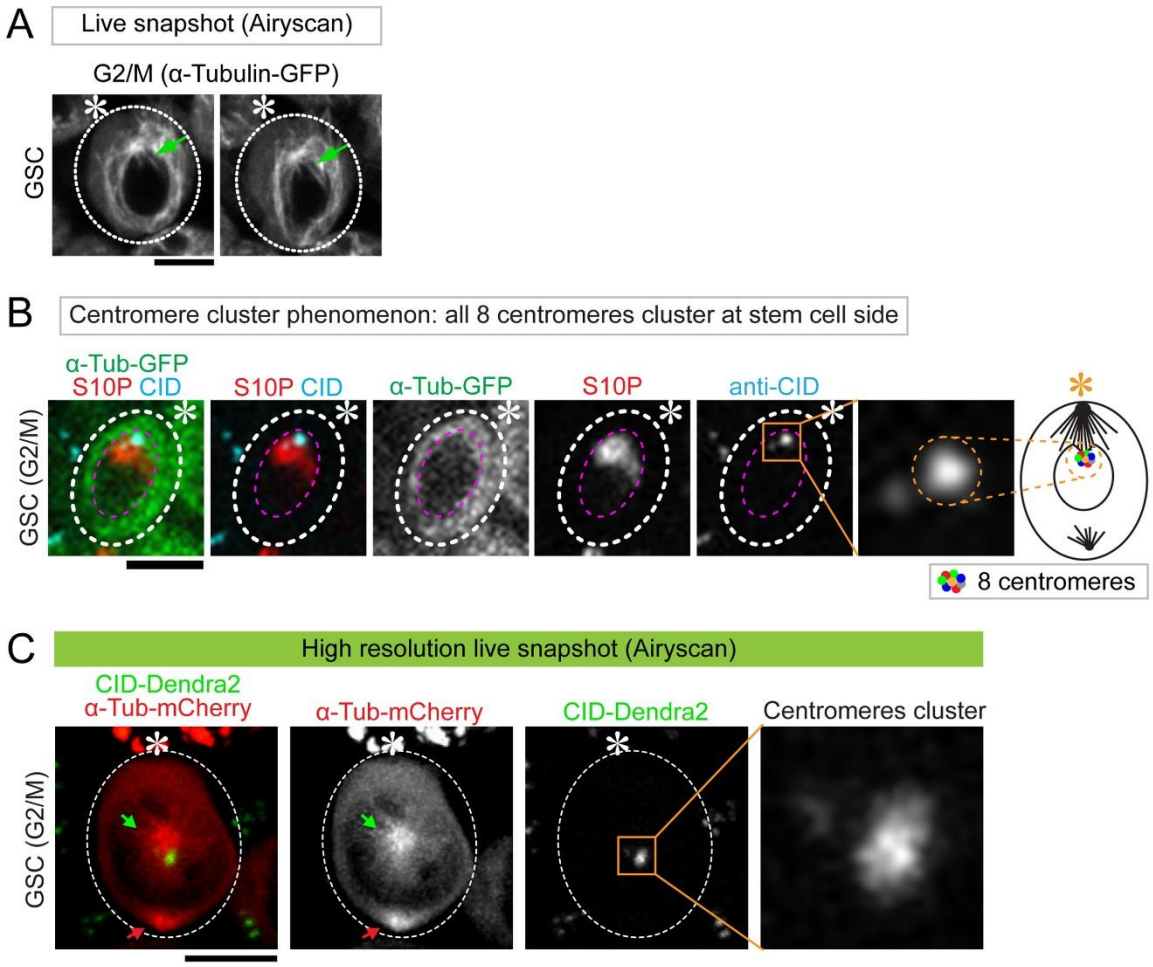

Figure S4. Related to Figure 4: Intimate interactions between microtubules and centromeres in GSCs. (**A**) The 'poking in' activities of microtubules from high resolution live cell Airyscan imaging, using the *nanos-Gal4*; *UAS-α-tubulin-GFP* line (snapshots from Movie S5). (**B**) A fix cell confocal image showing all CID signals (blue, centromeres from all chromosomes) were clustered near the nuclear envelope toward the niche side in GSCs at G2-to-M phase transition or prophase, with detectable H3S10P (red) and α-Tubulin signal (green). (**C**) A high resolution live snapshot (Airyscan) showing all CID signals (green, centromeres from all chromosomes) were clustered near the nuclear envelope toward the niche side in GSCs at G2-to-M phase transition or prophase, with mCherry-α-Tubulin signal (red). Asterisk: hub. Scale bars: 5μm.

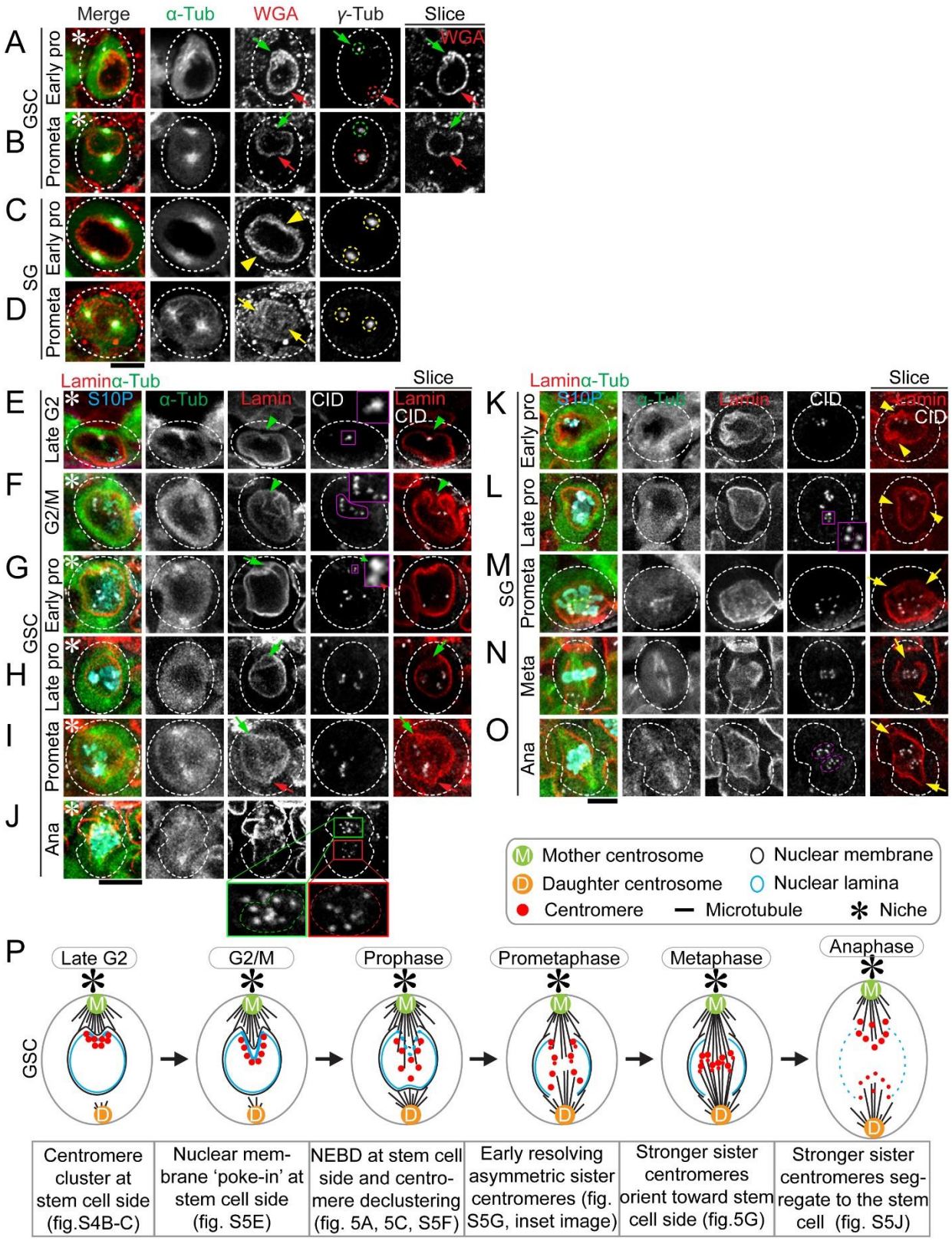
Merge
α-Tub
WGA
γ-Tub
Slice
A
Early pro
GSC
B
Prometa
C
Early pro
SG
D
Prometa
Laminα-Tub
Slice
E
Late G2
S10P
α-Tub
Lamin
CID
F
G2/M
G
Early pro
GSC
H
Late pro
I
Prometa
J
Ana
K
Early pro
L
Late pro
M
Prometa
SG
N
Meta
O
Ana
Mother centrosome
Daughter centrosome
Centromere
Nuclear membrane
Nuclear lamina
Microtubule
Niche
P
Late G2
G2/M
Prophase
Prometaphase
Metaphase
Anaphase
GSC
Centromere cluster at stem cell side (fig.S4B-C)
Nuclear membrane 'poke-in' at stem cell side (fig. S5E)
NEBD at stem cell side and centromere declustering (fig. 5A, 5C, S5F)
Early resolving asymmetric sister centromeres (fig. S5G, inset image)
Stronger sister centromeres orient toward stem cell side (fig.5G)
Stronger sister centromeres segregate to the stem cell (fig. S5J)

Figure S5. Related to Figure 5: Polarized NEBD in GSCs and a model for its potential role. (**A-D**) Morphology of nuclear envelope in GSCs (**A-B**) and SGs (**C-D**) at different cell cycle phases, visualized by wheat germ agglutinin (WGA, red) which binds to the cytoplasmic part of each nuclear pore, co-stained with anti-γ-Tubulin (white) in *nanos-Gal4*; *UAS-α-tubulin-GFP* line (α-Tub in green). The 'poking in' activities of microtubules are labeled by green arrows (from GSC side) and red arrows (from GB side) in (**A-B**). The interactions between microtubules and nuclear envelope in SGs are shown by yellow arrowheads at 'poking in' sites in (**C**) and yellow arrows at NEBD sites in (**D**). (**E-J**) Morphology of nuclear lamina at different cell cycle stages of GSCs, visualized by immunostaining with anti-Lamin B (red), co-stained with anti-CID (white) and anti-H3S10P (blue) in *nanos-Gal4*; *UAS-α-tubulin-GFP* (green) line. Polarized nuclear lamina invagination and centromere cluster at GSC side was labeled by green arrowheads from late G2 to G2/M transition (**E-F**). The 'poking in' activities of microtubules lead to centromere declustering along nuclear membrane (**F**). The 'poking in' activities of microtubules labeled by green arrow (from GSC side) at prophase to prometaphase and red arrow (from GB side) at prometaphase (**G-I**). Inset at early prophase shows a pair of resolved asymmetric sister centromeres (**G**). (**J**) Inset at anaphase show stronger sister centromeres segregated to the GSC side (green outlines), compared to the sister centromeres segregated to the GB side (red outlines). (**K-O**) Morphology of nuclear lamina at different cell cycle stages of SGs, visualized by immunostaining with anti-Lamin B (red), co-stained with anti-CID (white) and anti-H3S10P (blue) with the *nanos-Gal4*; *UAS-α-tubulin-GFP* (green) line. Nuclear lamina invagination was detected at both sides in SG labeled by yellow arrowheads at prophase (**K-L**). Inset at late prophase show two pairs of resolved symmetric sister centromeres (**L**). The 'poking in' activities of microtubules were from both poles labeled by yellow arrows at prometaphase

and metaphase (**M-N**). At anaphase, segregated sister centromeres show a symmetric pattern in SG (**O**). (**P**) A cartoon depicting the sequential events of the ‘mitotic drive’ in GSCs. Asterisk: hub. Scale bars: 5μm.

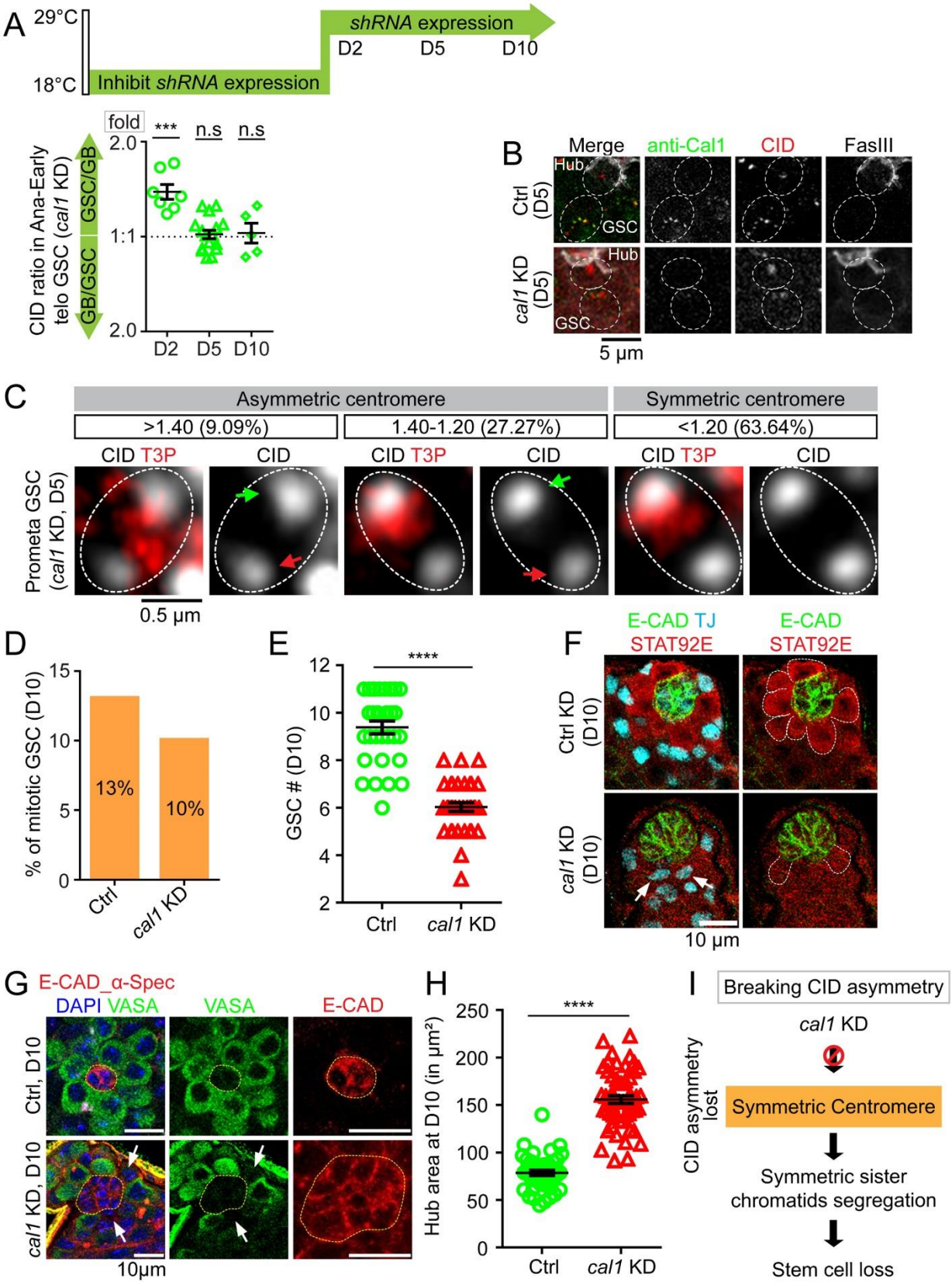
A
29°C
18°C
Inhibit shRNA expression
shRNA expression
D2
D5
D10
fold
***
n.s
n.s
CID ratio in Ana-Early telo GSC (cal1 KD)
GSC/GB
GB/GSC
2.0
1:1
2.0
D2
D5
D10
B
Merge
anti-Cal1
CID
FasIII
Ctrl (D5)
cal1 KD (D5)
Hub
GSC
5 μm
C
Asymmetric centromere
Symmetric centromere
>1.40 (9.09%)
1.40-1.20 (27.27%)
<1.20 (63.64%)
CID T3P
CID
Prometa GSC (cal1 KD, D5)
0.5 μm
D
% of mitotic GSC (D10)
13%
10%
Ctrl
cal1 KD
E
****
GSC # (D10)
Ctrl
cal1 KD
F
E-CAD TJ
STAT92E
E-CAD
STAT92E
Ctrl KD (D10)
cal1 KD (D10)
10 μm
G
E-CAD_α-Spec
DAPI VASA
VASA
E-CAD
Ctrl, D10
cal1 KD, D10
10μm
H
****
Hub area at D10 (in μm²)
Ctrl
cal1 KD
I
Breaking CID asymmetry
cal1 KD
CID asymmetry lost
Symmetric Centromere
Symmetric sister chromatids segregation
Stem cell loss

Figure S6. Related to Figure 6: Compromising CID asymmetry at sister centromeres by knocking down CAL1. (**A**) Gradual loss of asymmetric CID inheritance patterns in anaphase to early telophase GSCs from *cal1* KD testes two days (D2, *n*= 7), five days (D5, *n*= 11) or ten days (D10, *n*= 5) at the restrictive temperature (29°C). (**B**) The efficiency of *cal1* KD shown at D5 using immunostaining with anti-CAL1 (green) in *Ctrl* and *cal1* KD testes, co-stained with anti-CID (red) and anti-FasIII (hub cell marker). The anti-CAL1 immunostaining signal diminished in *cal1* KD GSCs compared to *Ctrl* GSCs. (**C**) Examples of resolved individual sister centromeres in *cal1* KD GSCs. In prometaphase GSCs, distribution patterns of CID at resolved individual sister centromeres in *cal1* KD GSCs at D5 showed different categories of asymmetry: highly asymmetric (> 1.40-fold, 9.1%) and medium asymmetric (between 1.2-1.4-fold, 27.3%), as well as symmetric pattern (<1.2-fold, 63.6%). Quantification also shown in Figure 6C-D (*n*= 33). (**D**) Mitotic index in *Ctrl* GSCs: 13.1% (42 H3S10P-positive GSCs/321 total GSCs) *versus* *cal1* KD GSCs: 10.1% (48 H3S10P-positive GSCs/476 total GSCs). (**E**) Quantification of the average number of GSCs per testis in *Ctrl* (9.44$\pm$ 0.25, *n*= 34), *cal1* KD (6.03$\pm$ 0.19, *n*= 35), Table S12. (**F**) Apical tip of testis from *Ctrl* KD and *cal1* KD males after knocking down *cal1* for ten days (D10), immunostained with anti-Stat92E (red), a somatic cell marker Traffic jam (Tj, cyan) and a hub marker *Drosophila* E-Cadherin (E-CAD, green). The empty niche place without GSCs is occupied by Tj-positive somatic cells labeled by white arrows in *cal1* KD testis. (**G**) Apical tip of testis from *Ctrl* KD and *cal1* KD males at D10, immunostained with a germ cell marker VASA (green), the hub marker E-CAD (red), and a spectrosome/fusome marker α-Spectrin (α-Spec, red). The empty niche place without GSCs is labeled by white arrows in *cal1* KD testis. (**H**) Hub area is indicated by yellow dotted outline in (**G**) and quantified: *Ctrl* (80.44$\pm$ 2.65μm^2, *n*= 45), *cal1* KD (155.88$\pm$ 4.05μm^2, *n*= 55), Table S15. (**I**) A cartoon shows loss of

sister centromere asymmetry by compromising CAL1 and the consequences of symmetric CID segregation, as well as stem cell loss. All ratios = Avg± SE. *P*-value: paired *t* test. ****: $P< 10^{-4}$; n.s: not significant. Asterisk: hub. Scale bars: 5μm (**B**), 0.5μm (**C**), 10μm (**F**-**G**).

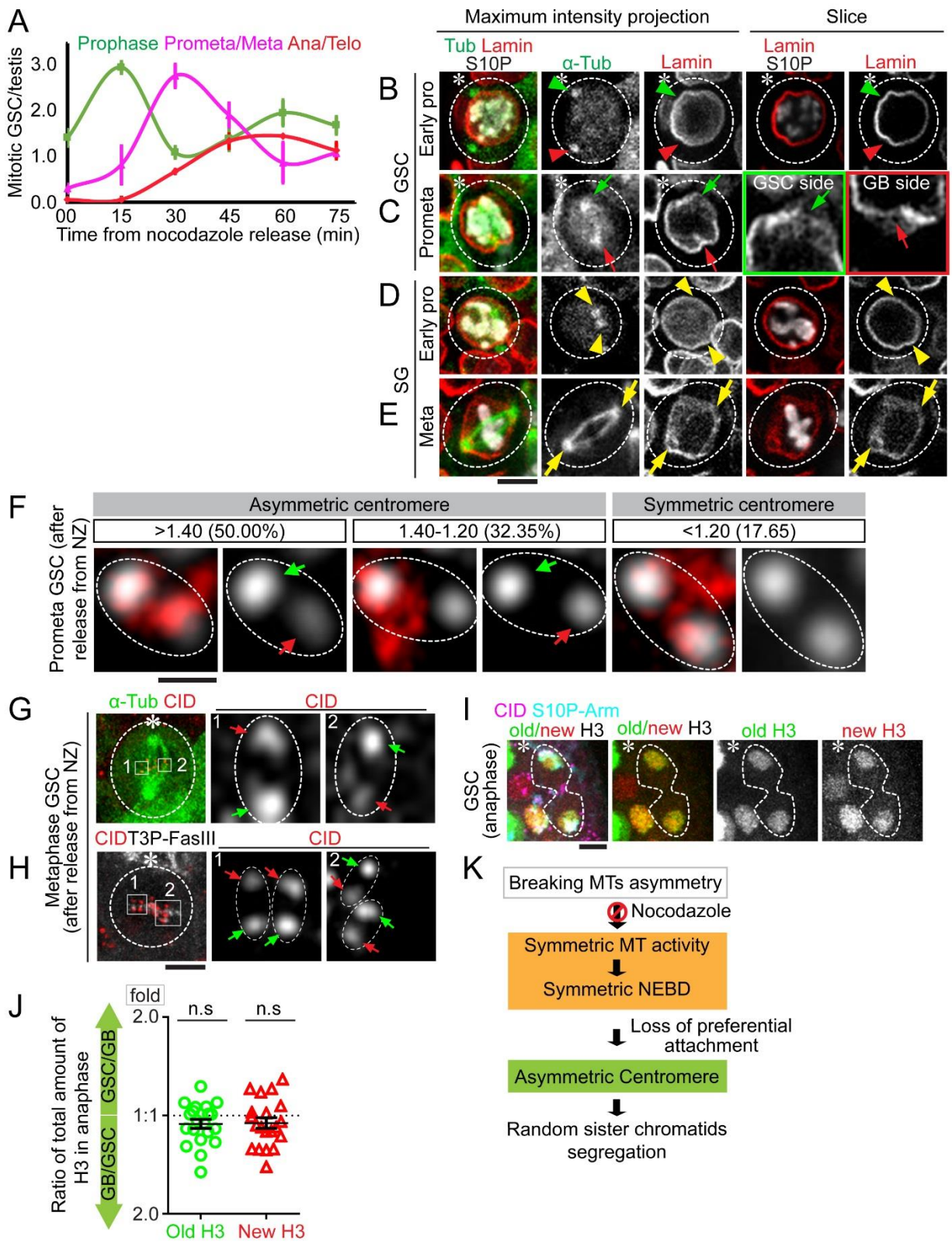
A
Prophase Prometa/Meta Ana/Telo
Mitotic GSC/testis
3.0
2.0
1.0
0.0
00 15 30 45 60 75
Time from nocodazole release (min)
Maximum intensity projection
Slice
Tub Lamin S10P
α-Tub
Lamin
Lamin S10P
Lamin
B
GSC
Early pro
C
Prometa
GSC side
GB side
D
SG
Early pro
E
Meta
F
Asymmetric centromere
Symmetric centromere
>1.40 (50.00%)
1.40-1.20 (32.35%)
<1.20 (17.65)
Prometa GSC (after release from NZ)
G
α-Tub CID
CID
Metaphase GSC (after release from NZ)
H
CIDT3P-FasIII
CID
I
CID S10P-Arm
old/new H3
old/new H3
old H3
new H3
GSC (anaphase)
J
fold
n.s
n.s
2.0
1:1
2.0
Ratio of total amount of H3 in anaphase
GB/GSC GSC/GB
Old H3
New H3
K
Breaking MTs asymmetry
Nocodazole
Symmetric MT activity
Symmetric NEBD
Loss of preferential attachment
Asymmetric Centromere
Random sister chromatids segregation

Figure S7. Related to Figure 7: Compromising microtubules asymmetry using nocodazole (NZ) treatment. (**A**) GSCs are primarily arrested at G2/M or early prophase with NZ treatment. Immediately after washing out NZ, GSCs progress to prophase after 15 minutes, prometaphase to metaphase after 30 minutes, and anaphase to telophase after 45 to 60 minutes. All time points = Avg± SE (*n*= 28 testes for t= 0 min, *n*= 22 testes for t= 15 min, *n*= 22 testes for t= 30 min, *n*= 24 testes for t= 45 min, *n*= 22 testes for t= 60 min, and *n*= 24 testes for t= 75 min). (**B-E**) Morphology of nuclear envelope visualized by immunostaining using anti-Lamin B (red), co-stained with anti-H3S10P (white) using *nanos-Gal4*; *UAS-α-tubulin-GFP* line (green): in GSCs at early prophase (**B**) and at prometaphase (**C**), when symmetric microtubule activity from both centrosomes could be visualized by α-Tubulin-GFP in GSCs after releasing from NZ-induced cell cycle arrest; in SGs at early prophase (**D**) and at metaphase (**E**). (**F**) Examples of sister centromeres in prometaphase GSCs immediately after releasing from NZ arrest. Distribution patterns of CID at resolved individual sister centromeres showed different categories of asymmetry: highly asymmetric (> 1.40-fold, 50.0%) and medium asymmetric (between 1.2-1.4-fold, 32.4%), as well as symmetric pattern (<1.2-fold, 17.6%). Quantification also shown in Figure 7E-F (*n*= 34). (**G-H**) Immediately after releasing from NZ arrest, sister chromatids with asymmetric sister centromeres are randomly attached by microtubules from mother centrosome *versus* daughter centrosome at the metaphase plate in two representative GSCs (**G** and **H**): examples include some stronger centromeres are attached to the microtubule emanating from the daughter centrosome (pattern 1 in **G-H**, green arrows) and some stronger centromeres are attached to the microtubule emanating from the mother centrosome (pattern 2 in **G-H**, green arrows). (**I-J**) Random histone H3 inheritance patterns in anaphase GSCs immediately after releasing from NZ-induced cell cycle arrest (**I**), as quantified in (**J**): old H3-GFP GSC/GB=

0.95± 0.03; new H3-mKO GB/GSC= 0.96± 0.04, (*n*= 20), Table S17. (**K**) A cartoon shows breaking asymmetric microtubules using NZ treatment and the consequences of random sister chromatids segregation. Ratio= Avg± SE; *P*-value: paired *t* test. ****: $P< 10^{-4}$; n.s: no significant difference. Asterisk: hub. Scale bars: 5μm in (**B-E**, **G-I**), 0.5μm in (**F**).